Soft Matter

Accepted Manuscript

ROYAL SOCIETY OF CHEMISTRY

www.rsc.org/softmatter

Submitted to *Soft Matter*

Wrapping/Unwrapping Transition of Double-Stranded DNA in DNA-Nanosphere Complexes Induced by Multivalent Anions

Aihua Chai[1,2], Yangwei Jiang[1], Yaoyang Zhang[3], Linli He[4], Dong Zhang[1], and Linxi Zhang[4, *)]

[1] *Department of Physics, Zhejiang University, Hangzhou, 310027, China*

[2] *College of Mathematics, Physics and Information Engineering, Jiaxing University, Jiaxing, 314001, China*

[3] *Department of Civil Engineering, Tsinghua University, Beijing 100084, China*

[4] *Department of Physics, Wenzhou University, Wenzhou , 325027, China*

Wrapping and unwrapping behaviors of a double-stranded DNA around a positively charged nanosphere in solution are studied by using the coarse-grained molecular dynamic (CGMD) simulation method. When monovalent, divalent and trivalent anions are added to the DNA-nanosphere complex solution, a double-stranded DNA is binding with a nanosphere owing to strong electrostatic attraction. However, when tetravalent anions are added to the DNA-nanosphere complex solution, local charge inversion is observed for a high anion concentration of tetravalent anions and the double-stranded DNA can be unwrapped from the nanosphere because of the local charge inversion near the nanosphere. Moreover, the helical structure of DNA is damaged when double-stranded DNA is wrapping around the nanosphere and the helical structure can be rebuilt when the double-stranded DNA is unwrapping from the nanosphere. This study can help us understand how to control the release of DNA in DNA-nanosphere complexes.

* Corresponding author. E-mail: lxzhang@zju.edu.cn.

I. Introduction

A DNA-nanoparticle plays an important role in fundamental life processes because its dynamic organization is a key factor for controlling the regulation of gene expression such as replication, transcription, repair and recombination.[1] Some novel technologies based on DNA-nanoparticle interactions have been used in molecular diagnosis, sensing and gene therapy. These approaches can offer an opportunity for the development of efficient and low-cost technologies for disease diagnosis and DNA detection with high sensitivity.[2] Nanoparticles (NPs) can be chosen as desirable carriers of DNA in target delivery because DNA can overcome the drawbacks of using liposomes due to their inherent problems such as rapid leakage in blood and poor storage stability. A DNA-nanoparticle complex is regarded as an efficient model to reveal fundamental mechanisms of the natural packing of DNA by histone octamers. In eukaryotic cells, DNA is organized into chromatin. Its basic packing unit is a nucleosome core particle, which wraps 146 base pairs of DNA around a protein complex. It seems that complexes of DNA with oppositely charged objects such as nanoparticles in vitro are promising as model systems to reveal fundamental mechanisms of the natural packing of DNA by histone octamers. The fact that DNA wraps around nanoparticles and is packaged into a smaller volume to fit in cells is an important strategy to protect the genetic information from external factors.[3]

To understand the DNA-nanoparticle binding and its principal molecular interaction mechanism is a subject of great interest in biology. In recent decades, many studies about DNA compaction by proteins,[4] dendrimers[5,6] and nanoparticles[7-14] have been done. For example, Li *et al.* found that the short single-stranded DNA could bind to 13 nm Au-NP , and ssDNA and dsDNA have different propensities to be adsorbed on Au-NPs because of their electrostatic properties.[15] Cao *et al.* investigated the interaction of a double-stranded DNA with a nanosphere and found that DNA could wrap randomly around a nanosphere only at an intermediate salt concentration and high surface charge density.[16] McIntosh and coworkers found that using cationic mixed monolayer protected gold clusters (MMPCs) could inhibit DNA transcription.[17] Stoll and Chodanowski studied the formation of complexes between flexible, semiflexible, and rigid polyelectrolyte and

an oppositely charged spherical nanoparticle by means of Monte Carlo simulations, and found that the critical ionic concentration at which adsorption/desorption is observed rapidly decreases with the polyelectrolyte intrinsic rigidity.[12] In fact, it is known that the wrapping behavior of DNA in cells is influenced by the tension generated by molecular motors.[18,19] In a real nucleosome, the tight wrapping of DNA around the histone should limit the accessibility of transcriptional factors, and the nucleosome structure in genetically active state is expected to be loosened or, at least, partially unwrapped.[2] Many researches focus on the response of the DNA-nanoparticle complexes with respect to an external force acting on DNA chains.[20,21] Sakaue and Löwen studied the unwrapping process of DNA-protein complexes by computer simulations and simple phenomenological theory,[22] and found that, for a flexible chain, the sphere-chain complex is disordered and the extension of the complex scaled linearly with the external force applied. For a stiff chain, on the other hand, the complex structure is ordered. In fact, in gene therapy, DNA is rapidly degraded before reaching the target if the naked DNA is directly delivered. Guo *et al.* found that Au-NP and carbon nanotubes (CNTs) could be used as effective non-viral vectors to overcome those obstacles in transporting plasmid DNA, siRNA or antisense oligonucleotides because the use of viral vectors to deliver DNA may cause some problems, for example, they may produce a serious immune response in the host, which can be lethal and endanger patients.[23] In fact, the effective delivery includes protection of biomolecules such as nucleic acid from degradation by nuclease as well as release of the nucleic acid in a function form[24]. Therefore, how to unwrap DNA from a nanoparticle is an interesting issue in biology.

In this work, we investigate the conformations of the complexes with double-stranded DNA and an oppositely charged nanosphere in multivalent anion solutions using coarse-grained molecular dynamic (CGMD) simulation method. The wrapping/unwrapping behavior of DNA from a nanosphere is observed by adding tetravalent anions into the solutions (here a nanoparticle with a large size is called as a nanosphere). The helical structure of DNA is damaged when it wraps around a nanosphere, and the helical structure can be rebuilt when DNA is unwrapped from a nanosphere. The study can help us understand how to control the release of DNA in DNA-nanoparticle complexes.

II. Model and simulation method

In our molecular dynamic (MD) simulation, we use the Biochemical Algorithms Library[25] to build the double-stranded DNA model, which is based on representing each DNA base-pair by two monomers of the same type, where each monomer is placed in the geometric center of the corresponding base-pair nucleotide. As one nucleotide is replaced by one monomer, the number of atoms decreases greatly for a DNA chain in our model. For example, the molecular formula for guanine (G) is $C_5H_5N_5O$, and the number of atoms is 16. In our CG model of DNA, one monomer represents the whole guanine of $C_5H_5N_5O$, therefore, our model can lead to an ~30-fold reduction of DNA degrees of freedom while fan interactions can preserve the major and minor groove structural patterns.[26] In our system, the total number of base-pairs in each double-stranded DNA is $N_D = 50$ and each monomer carries a unit negative charge $q_i = -e$, where e is the elementary charge. The nanosphere is modeled via a fishnet-like network.[27,28] In our model, a nanosphere is made up of 642 monomers, and 162 monomers are positively charged with the total charges of 324*e* (i.e., $162 \times 2e$), which are uniformly distributed on the spherical surface. As the system consists of a number of multivalent anions and cations, this leads to more electrostatic screening and in turn weakens the electrostatic attraction between nanosphere and DNA, therefore, it is necessary to load enough charges on the nanosphere surface. If only a few charges are distributed on the spherical surface, the wrapping behavior can not occur because of weak electrostatic attraction in multivalent anion solution.[20] The radius of nanosphere is $R_s = 16\sigma$ in our model.

In the coarse-grained model, all of the four types of DNA nucleotides are replaced with identical monomer units. The potential of double-stranded DNA chains is defined as the following polynomial forms[26]:

$$U_{DNA} = U_{bond} + U_{angle} + U_{helix} \tag{1}$$

The individual energetic contributions to this potential are given by:

$$U_{bond} = K_2^b (l - l_0)^2 + K_3^b (l - l_0)^3 + K_4^b (l - l_0)^4 \tag{2}$$

$$U_{angle} = K_2^a(\theta - \theta_0)^2 + K_3^a(\theta - \theta_0)^3 + K_4^a(\theta - \theta_0)^4 \quad (3)$$

$$U_{helix} = K_2^h(l - l_0^{'})^2 + K_3^h(l - l_0^{'})^3 + K_4^h(l - l_0^{'})^4 \quad (4)$$

where U_{bond} and U_{angle} denote intra-strand interactions for bond and bending angle potential energies, respectively. U_{helix} is a nonstandard fan interaction and is responsible for maintenance of the DNA double-strand, which is formed by two polynucleotides.[26] Here, the values of l_0 and θ_0 are the bond equilibrium length and the equilibrium angle in each DNA strand, respectively, and $l_0^{'}$ is the equilibrium interaction separation for fan interaction.[26] In our DNA coarse-grained model, fan interactions indicate interactions between a given monomer located on one strand and a number of monomers located on the other strand, and there are 11 such interactions associated with base-pairing and stacking of two polynucleotides[26]. The equilibrium values l_0, $l_0^{'}$, and θ_0, as well as the interaction parameters K_α^b, K_α^a, and K_α^h (α=2, 3, and 4) are extracted from all-atom (AA) and coarse-grain (CG) MD simulations.[25,26,29]

We describe nanosphere inter-monomer interactions with the following potential:[28,30]

$$U_s = -\frac{1}{2}Kl_{0s}^{\ 2}\ln\left[1-\left(\frac{r_{ij}}{l_{0s}}\right)^2\right] + K_b(1+\cos\Phi) \quad (5)$$

where the first term is a finite nonlinear extensible elastic (FENE) potential describing for neighboring monomer interaction and the second term is a bending potential imposed between all neighboring triangular faces. The parameter $K = 30\varepsilon$ denotes the spring constant and $l_{0s} = 4.5\sigma$ is the maximum bond length allowed. The reduced units $\varepsilon = k_BT = 1$ and $\sigma = 1$ Å are used, where k_B is Boltzmann constant, and T is the temperature. Φ is the dihedral angle between opposite vertices of any two triangles sharing an edge, and $K_b = 1000\varepsilon$ is used to maintain the spherical shape of the nanosphere.

Finally we model the excluded volume interactions between all monomers in the system through the combination of Coulomb interaction and Lennard-Jones (LJ) potential.

$$U_{eCLJ} = \frac{q_i q_j}{4\pi\varepsilon_0\varepsilon_r r_{ij}} + 4\varepsilon\left[(\frac{\sigma^*}{r_{ij}})^{12} - (\frac{\sigma^*}{r_{ij}})^6\right] \quad (6)$$

where the first term is the electrostatic interactions between all intermolecular pairs of charges, q_i and q_j are the charges of monomers i and j, ε_0 is the permittivity of vacuum and $\varepsilon_r = 10$ is the relative dielectric constant of the solvent, r_{ij} is the distance between the centers of monomers i and j. The second term is a single Lennard-Jones potential with a cut distance $2^{1/6}\sigma^*$ between any two monomers.[31,32] To avoid overlap, the Lennard-Jones potential written in Eqn (6) is also applied to all the monomers with various diameters of DNA monomer $\sigma^*_{dna} = 5.0\sigma$ =5.0Å, and the other monomer such as anions and cations $\sigma^*_{other} = 3.0\sigma$ =3.0Å, and the parameters are given by the mixing rules: $\varepsilon_{ij} = \sqrt{\varepsilon_i\varepsilon_j} = \varepsilon$ and $\sigma^*_{ij} = (\sigma^*_i + \sigma^*_j)/2$ (*i, j= dna, other*).

We study the wrapping/unwrapping behavior of double-stranded DNA in DNA-nanosphere complex solutions by using the open source software LAMMPS molecular dynamics package[33] with a Nosé-Hoover thermostat[34,35] in the NVT ensemble. In our simulation, it is assumed that the mass of the monomers is identical, $m = 1$, and the temperature is set to be $T = 1.2$. The friction coefficient γ and the timestep are $\gamma = 1/\tau_0$ and $\tau = 0.001\tau_0 = 0.1ps$, respectively, where $\tau_0 = \sqrt{m\sigma^2/\varepsilon}$ is the time unit in our simulation. At the same time, each simulation runs at least 2×10^7 steps in the periodic box $176\sigma\times176\sigma\times176\sigma$ with periodic boundary conditions in three directions. The Coulomb interactions are handled by the particle-particle particle-mesh (PPPM) method.[36-38] We investigate the statistical properties of DNA-nanosphere complexes in solvents by varying the number of monovalent M^{1-}, divalent M^{2-}, trivalent M^{3-}, and tetravalent M^{4-} anions. For the sake of preserving the neutrality of the whole system, a number of cations (i.e., counterions), such as monovalent cations M^{1+}, are added to the solution. The anion concentration C_s is used to represent the salt concentration, which varies from 30.5 to 91.5 mM, corresponding to the number of anions from 100 to 300. Various anion and cation concentrations used in our simulations are given in detail in the Supplementary Information.

Submitted to *Soft Matter*

III. Results and discussion

A. Unwrapping behavior of double-stranded DNA

As we know, DNA exhibits one intrinsic negative charge because its sugar-phosphate backbone can be adsorbed on a positively charged spherical surface.[16] When a varying number of tetravalent anions are added to the DNA-nanosphere complex solutions, it is found that the unwrapping process of double-stranded DNA from a nanospherical surface can be induced by tetravalent anions. Fig. 1 gives typical simulation snapshots of the DNA-nanosphere complexes in monovalent, divalent, trivalent, and tetravalent anion solutions. The conformations of DNA-nanosphere complexes depend on the type of multivalent anions, as well as the anion concentration (C_s). In the monovalent anion solution, as shown in the first row in Fig. 1, double-stranded DNA wraps around a nanosphere tightly in spite of the anion concentration increasing from C_s =30.5mM to 91.5mM. In the divalent anion solution, the conformations of DNA-nanoparticle complex solutions are almost the same as the monovalent anion solution, as shown in the second row in Fig. 1. The third row in Fig. 1 shows that DNA wraps loosely around a nanosphere. The most interesting phenomenon occurs in the tetravalent anion solution, as shown in the fourth row in Fig 1. It is observed that double-stranded DNA is unwrapped slowly from a nanosphere by increasing the anion concentration. When C_s =91.5mM, DNA can be unwrapped from the nanospherical surface completely. Wrapping/unwrapping transition of DNA in a DNA-nanosphere complex is very important in gene therapy and drug delivery because an effective gene delivery for nanosphere includes non-covalent DNA-nanosphere binding and effective control for the release of DNA in gene therapy or regulation.[2,23,24] In fact, non-covalent DNA-nanosphere binding means wrapping behavior of DNA, and the release of DNA in gene therapy or regulation represents unwrapping process of DNA. Although unwrapping of DNA in DNA-nanosphere complexes has been investigated by using steered molecule dynamics method, [16,39] and optical tweezers,[40] the external force acting on DNA directly in steered molecular dynamics simulation or optical tweezers experiments always can't be implemented *in vivo*. Therefore, unwrapping behaviors of DNA in DNA-nanosphere complexes induced by tetravalent

anions can help us understand how to control the release of DNA in DNA-nanosphere complexes because the driving force of wrapping/unwrapping transition comes from the solution itself.

We describe the wrapping degree of DNA by using the percentage of double-stranded DNA monomers wrapping around a nanosphere ($< P >$), and the results are shown in Fig. 2. The DNA monomers whose distance away from the nanosphere surface is less than 10σ are regarded as the wrapping monomers here. For monovalent and divalent anions, DNA wraps around a nanosphere and <P> decreases a little from 96% to 86% when the anion concentration C_s varies from 0 to 91.5mM. But for trivalent anions, <P> decreases to 70% for C_s =91.5mM. For tetravalent anions, <P> decreases abruptly from 96% to 12% when C_s increases from 0 to 91.5mM, which indicates that the double-stranded DNA has been away from a nanosphere completely. To quantify the size of the double-stranded DNA in the solutions clearly, we calculate the characteristic ratio of mean-square radius of gyration $< R_G^2 > / N_D l_0^2$ and the shape factor $< \delta >$, where N_D (=50) is the number of monomers per DNA strand and l_0 is the DNA bond length. The shape factor of DNA can be obtained by combing the reduced components of S^2 to a single quantity[41-44]

$$< \delta >= 1 - 3 < \frac{L_1^2 L_2^2 + L_1^2 L_3^2 + L_2^2 L_3^2}{(L_1^2 + L_2^2 + L_3^2)^2} > \qquad (7)$$

The "equivalent ellipsoid" of a configuration can be obtained by evaluating the principal components $L_1^2 \geq L_2^2 \geq L_3^2$ of the squared radius of gyration and $S^2 = L_1^2 + L_2^2 + L_3^2$ of individual configurations are taken along the principal axes of inertia.[41-44]The results are shown in Fig. 3. The characteristic ratio of $< R_G^2 > / N_D l_0^2$ and the shape factor $< \delta >$ increases a little when C_s increases from 0 to 91.5mM for monovalent, divalent and trivalent anions. The reason is that the conformations of double-stranded DNA remain unchanged when we vary the anion concentration. However, the values of $< R_G^2 > / N_D l_0^2$ and $< \delta >$ increase abruptly from $< R_G^2 > / N_D l_0^2$ =0.50 to 1.88 and from $< \delta >$=0.13 to 0.93 respectively when C_s for tetravalent anions increases from 0 to 91.5mM. $< \delta >$=0.93 means that the shape of double-stranded DNA becomes rod-like, and double-stranded DNA can be unwrapped from the positively charged nanosphere by increasing the tetravalent anion concentration. However, the double-stranded DNA

Submitted to *Soft Matter*

still wraps around the nanosphere when a number of monovalent, divalent, and trivalent anions are added to the DNA-nanosphere complex solutions.

The helical structure of double-stranded DNA may be damaged when wrapping/unwrapping transition occurs when tetravalent anions are added to the DNA-nanosphere complex solutions. To characterize the helical structure, we calculate the correlation functions between the tangent vectors $\vec{u}(1)\cdot\vec{u}(s)$,[45,46] where $\vec{u}(1)$ and $\vec{u}(s)$ are tangent vectors for monomers 1 and s in double-stranded DNA. Fig. 4 shows $\vec{u}(1)\cdot\vec{u}(s)$ as a function of DNA monomers s for DNA-nanosphere complex solutions with different multivalent anions. In order to have a preliminary reference, we also plot $u(1)\cdot u(s)$ of an isolated double-stranded DNA in the solution, in which there are a DNA and a few cations for preserving the neutrality of the whole system, (see Fig.4a). The periodic oscillation with the same magnitude indicates that the isolated double-stranded DNA has perfect helical structure. For the tetravalent anion (M^{4-}) solution with C_s =30.5mM, the curve of $\vec{u}(1)\cdot\vec{u}(s)$ (circle line) fluctuates within a large amplitude without any periodicity at all. This result suggests that the DNA helix has been damaged seriously. In the case of C_s =61.0mM, the $\vec{u}(1)\cdot\vec{u}(s)$ shows a certain periodicity but is not very good, as shown in Fig.4a. However, the curve of $\vec{u}(1)\cdot\vec{u}(s)$ exhibits periodic oscillation again with the same magnitude for C_s =91.5mM. It indicates that the helical structure of DNA can be rebuilt in high anion concentration of tetravalent anion solution. Fig. 4b shows the values of $\vec{u}(1)\cdot\vec{u}(s)$ for various anions with a fixed anion concentration C_s =91.5mM, and $\vec{u}(1)\cdot\vec{u}(s)$ shows a periodic oscillation only for the tetravalent anion. Moreover, the dihedral angle of double-stranded DNA θ can also be used to characterize the helical structure of double-stranded DNA. As shown in Fig. 5, the consecutive dihedral angles are all around 2.67 (153^o) for isolated double-stranded DNA (square line). For the tetravalent anion solution with C_s =30.5mM, the dihedral angles fluctuate within a large amplitude, which indicates that the helical structure of DNA has been damaged partly. When C_s increases, the fluctuating amplitude of dihedral angles decreases and the helical structure can be kept well, see Fig.5.

In order to explore the helical structure of double-stranded DNA in more detail, we calculate

the orientational correlation function $G(m)$[47], which is defined as

$$G(m)=\frac{1}{N-3}\sum_{i=2}^{N_D-2}g(m,i) \tag{8}$$

where

$$g(m,i)=\frac{\sum_{j=1}^{N_D-m-1}(cos\varphi_{i,j}-\overline{cos\varphi_{i,j}})(cos\varphi_{i,j+m}-\overline{cos\varphi_{i,j}})}{\sum_{j=1}^{N-1}(cos\varphi_{i,j}-\overline{cos\varphi_{i,j}})^2}. \tag{9}$$

The angle is defined as

$$\cos\varphi_{i,j}=\frac{\vec{l}_i\cdot\vec{l}_j}{|\vec{l}_i|\cdot|\vec{l}_j|}. \tag{10}$$

where m means monomer interval, which ranges from 0 to $\frac{N_D}{2}-1$. $\overline{\cos\varphi_{i,j}}$ denotes the average of $\cos\varphi_{i,j}$ over j from 1 to N_D-1. $\vec{l}_i$ is a bond vector which indicates the vector connecting monomer i to monomer i+1; and φ_i is the angle between $\vec{l}_{i-1}$ and $\vec{l}_i$. In Fig. 6, the curve of G(m) oscillates uniformly for the isolated double-stranded DNA (square line), while the other parts oscillate non-uniformly except for the inverted triangle line. It means that only in the high concentration of tetravalent anions solution can the double-stranded DNA keep its helical structure. From the above analysis, we believe that DNA can be unwrapped from the positively charged nanospherical surface by increasing the salt concentration of tetravalent anions in the DNA-nanosphere complexes. Although the DNA chain used here is the coarse-grained model, our results agree with the results based on the all-atomistic model of DNA chains.[48] Of course, if the all-atomistic model of DNA chains is adopted, some new results can be obtained, for example, two polynucleotides may be broken off when DNA wraps around the nanosphere tightly in the DNA all-atomistic model, while two polynucleotides are always linked through bonds in the coarse-grained model.

B. Electric characteristics of nanospherical surface

Submitted to *Soft Matter*

To obtain the inherent mechanism of unwrapping behavior of double-stranded DNA, we calculate the integrated charge distribution, $Q_e(r)$, which is defined as the mean total charge density of particles including anions, cations, DNA monomers, and positive charges inside a sphere, the origin of which is the center of the nanosphere, with radius equal *r*. In Fig. 7a, the value of $Q_e(r)$ is zero for $r<16\sigma$ because there are no charges inside a nanosphere. All the curves reach their maxima at $r=16\sigma$ because the nanospherical surface is positively charged. With the increase of *r*, the profiles decrease by the contribution of the added multivalent anions, especially for tetravalent anions. This negative $Q_e(r)$ in some regions such as $24<r<35$ and $39<r<46$ for tetravalent anions indicates some charge inversion regions are created. In fact, this is the charge inversion phenomenon, which is very interesting in colloid and surface science[49-51] and has potential relevance to the development of biological applications such as gene delivery.[52] Compared with other lines in Fig. 7a, the line for tetravalent anions (M^{4-}) has four overcharging regions while there are no regions with $Q_e(r)<0$ for monovalent and divalent anions, which means that the charge inversion phenomenon can't occur for M^{1-} and M^{2-}. The inset figure in Fig. 7a gives $Q_e(r)$ for tetravalent anion solution when the anion concentration C_s is varied. It is observed that the charge inversion phenomenon is more obvious for tetravalent anions with the high anion concentration of C_s =91.5mM. Of course, $Q_e(r)$ is close to zero in the limit of $r\to\infty$ because of the neutrality of the solvent. Namely, the more anions the solvent includes, the more opposite charges the surface can absorb. In order to explore the reason why the wrapping/unwrapping transition of DNA can occur in multivalent anions, we also study the charge distribution around the nanoparticle in the multivalent anion solutions without any DNA molecules, providing the reference states for the more complicated complexes. The result in Fig. 7b shows that there is no charge inversion region in monovalent and divalent anion solutions, and a large charge inversion region in tetravalent anion solution. Therefore, it is charge inversion phenomenon in a DNA-nanosphere complex solution that causes the DNA unwrapping from the nanosphere.

To further study the charge spatial distribution on the nanospherical surface, we calculate the

integrated surface charge density σ_e in the local sphere shell. A DNA is located at $\phi \approx 0^\circ$ in spherical coordinate and σ_e is the integrated surface charge density in the local sphere shell whose angle is from $\phi - 18^\circ$ to $\phi + 18^\circ$ and whose radius is less than 26σ, see Fig 8a. Then, the sphere shell is divided into 10 parts uniformly according to the azimuth angle ϕ. In the monovalent anion solution, all values of σ_e are greater than zero and have only a few fluctuations, as shown in Fig. 8b (b1, C_s =30.5mM) and (b2, C_s =91.5mM). This indicates that the nanosphere is still positively charged, the distribution of positive charges near the nanosphere is uniform, and DNA can be adsorbed on the nanospherical surface through the electrostatic attraction, see the inset figure in Fig. 8b. However, in the tetravalent anion solution, the integrated surface charge densities σ_e in some shell regions are less than zero and the distributions of σ_e are non-uniform. In the case of C_s =30.5mM, the negative charges σ_e are mainly located at $\phi = 180^\circ \pm 90^\circ$, which is completely opposite to the position of DNA ($\phi = 0^\circ$). The negative charges exist in five regions, and half of sphere shell is full of positive charges. DNA can still wrap around the nanosphere though the compact degree between DNA and a nanosphere in the tetravalent anion solution is different from that in the monovalent anion solution, see the inset figure in Fig 8(c1). When the tetravalent anion concentration increases to C_s =91.5mM, most parts of sphere shell are negatively charged. The more tetravalent anions are close to the nanospherical surface, the more obviously the nanosphere exhibits being negatively charged, and the negative charges are located mainly from $\phi = 54^\circ$ to $\phi = 306^\circ$, therefore, DNA can be unwrapped from the nanosphere, as shown in Fig.8 (c2).

What is the inherent mechanism for the unwrapping of DNA from the nanosphere? We investigate the simulation process of the tetravalent anion solution with a fixed concentration C_s =91.5mM, with the results shown in Fig 9(a). After a short simulation time (such as t=$10000\tau_0$), DNA is binding tightly with the nanosphere because of strong electrostatic attractive interaction between the DNA and the nanosphere, and only few tetravalent anions can be adsorbed near the nanosphere. Then, some tetravalent anions move towards the nanosphere because there exists the

Submitted to *Soft Matter*

relatively strong attractive interaction between high-valence anions and the nanosphere, however, the spatial distribution of tetravalent anions near the nanosphere is non-uniform, see Fig 9(a)-(a2-a3). The reason may be that on the one hand, some tetravalent anions aggregation can lead some DNA monomers to be unwrapped from the nanosphere partly, one the other hand, it is difficult for the tetravalent anions to move towards the regions near the nanosphere where some DNA monomers have been wrapped because there are the repulsive interactions between DNA monomers and tetravalent anions. After a long period of equilibrium, more tetravalent anions are aggregated in the region which is located at $\phi = 180^{\circ}$, and the unwrapping of DNA from the nanosphere can be induced by these strongly repulsive electrostatic interactions. The quantitative investigations about unwrapping behavior of DNA in DNA-nanosphere complexes are performed, and the results are shown in Fig 9(b). Here the total deviation of integrated surface charge density *A* is defined as

$$A = \sum_{i=1}^{10} (\sigma_{e,i} - < \sigma_e >)^2 \tag{11}$$

Where $\sigma_{e,i}$ is the surface charge density in the *i*-th local sphere shell, *i* is from 1 to 10 (see Fig 8(a)), and $< \sigma_e >$ is the average value. Different conformations of DNA in DNA-nanosphere complexes at different simulation time can produce different values of *A*. As shown in Fig. 9(b), in monovalent (square line) and divalent (circle line) anion solutions, the values of *A* are very small, which indicates that the surface charge density distribution near the nanosphere is uniform. However, in the tetravalent anion solution, the value of *A* keeps small at $t < 4.5 \times 10^5$ because the charges can keep the uniform distribution before this time. After a long simulation time, the local tetravalent anion aggregation can bring about a large deviation of integrated surface charge density, i.e., a very large value of *A*, see Figs 9(a)-a4 and 9(b).

Of course, the effects of the additional cations, which are used to neutralize the system, should be considered. Typical snapshots of DNA-nanosphere complexes with the same cation concentration of $C_S^{'}$=464.4mM for monovalent, divalent, trivalent, and tetravalent anions are shown in Fig 10. Obviously, only in the tetravalent anion solution, the DNA can be unwrapped from a nanosphere completely for the same cation concentration. From the above results, we can

conclude that tetravalent anions can change the electrical characteristics of the nanospherical surface and induce the unwrapping of DNA from nanospheres.

IV. Conclusions

In this paper, we investigate the wrapping/unwrapping behaviors of double-stranded DNA in DNA-nanosphere complexes in the presence of various anions by performing a series of CGMD simulations. In the high concentration tetravalent anion (M^{4-}) solutions, the nanospherical surface is easy to be oppositely charged, and DNA can be unwrapped from the nanosphere because of the repulsive electrostatic interactions. However, in the monovalent and divalent anion solutions, the nanosphere surface can't be oppositely charged, so DNA always wraps around the nanosphere. Moreover, it is observed that the helical structure of DNA is damaged when DNA wraps around the nanosphere. An interesting phenomenon is observed that the helical structure of DNA can be rebuilt when it is unwrapped from the nanosphere induced by the added tetravalent anions. Wrapping/unwrapping transition of DNA in DNA-nanosphere complexes induced by tetravalent anions in solutions can help us understand how to control the release of DNA in DNA-nanosphere complexes.

Acknowledgments

This research was financially supported by the National Natural Science Foundation of China (Nos. 21374102, 20934004, 21174131, 21104060). We are grateful to the reviewers of our manuscript for their detailed and insightful comments and suggestions.

References

1. R. Saecker and M. Record, *Curr. Opin. Struct. Biol.,* 2002, **12**, 311.
2. H. An and B. Jin, *Biotechnol. Adv.* 2012, 30, 1721–1732.
3. K. van Holde and J. Zlatanova, *Semin. Cell Dev. Biol.*, 2007, **18**, 651.
4. C. A. Davey, D. F. Sargent, K. Luger, A. W. Maeder and T. J. Richmond, *J. Mol. Biol.*, 2004, **319**, 1097.
5. A. U. Bielinska, J. F. Kukowska-Latallo and J. R. Baker, *BBA*, 1997, **1353**, 180.
6. A. U. Bielinska, C. Chen, J. Johnson and J. R. Baker, *Jr., Bioconj. Chem.*, 1999, **10**, 843.
7. K.-K. Kunze and R. R. Netz, *Phys. Rev. Lett.*,2000, **85**, 4389.
8. L. Zhang and Y. X. Zhu., *Soft Matter*, 2009, **5**, 4290.
9. R. Mahtab, H. H. Harden and C. J Murphy, *J. Am. Chem. Soc.,* 2000, **122**, 14.
10. R. Messina, *J. Chem. Phys.,* 2002, **117**, 11062
11. R. R. Natz and J. F. Joanny, *Macromolecules*, 1999, **32**, 9026.
12. S. Stoll and P. Chodanowski, *Macromolecules*, 2002, **35**, 9556.
13. A. G. Cherstvy and R.G. Winkler, *J. Phys. Chem. B*, 2012, 116, 9838.
14. M. M. Hatlo and L. Lue, *Soft Matter*, 2008, 4, 1582
15. H. X. Li and L. Rothberg, *Proc. Natl. Acad. Sci. U. S. A.*, 2004, **101**, 14036.
16. Q. Q. Cao, C. C. Zuo, Y. H. Ma, L. J. Li and Z. Zhang, *Soft Matter*, 2011, **7**, 506.
17. G. M. McIntosh, E. A. Esposito, III, A. K. Boal, J. M. Simard, C. T. Martin and V. M. Rotello, *J. Am. Chem. Soc.*, 2001, **123**, 7626.
18. P. Cook, *Science*, 1999, **284**, 1790.
19. S. Leuba, M. Karymov, M. Tomschik, R. Ramjit, P. Smith, and J. Zlatanova, *Proc. Natl. Acad. Sci. U.S.A.*, 2003, **100**, 495.
20. K.-K. Kunze and R. R. Netz, *Phys. Rev. E*, 2002, **66**, 011918.
21. I. Kulić and H. Schiessel, *Phys. Rev. Lett.*, 2004, **92**, 228101.
22. T. Sakaue and H. Löwen, *Phys. Rev. E*, 2004, **70**, 021801.
23. S. Guo, Y. Huang, Q. Jiang, Y. Sun, L. Deng, Z. Liang, *ACS Nano.*, 2010, **4**, 5505.

24. G. Han, P. Ghosh, M. De, V. Rotello, *Nanobiotechnology*, 2007, **3**, 40.
25. O. Kohlbacher and H. P. Lenhof, *Bioinformatics,* 2000, **16**, 815.
26. A. Savelyev and G. A. Papoian, *Biophys. J.*, 2009, **96**, 4044.
27. G. A. Vliegenthart and G. Gompper, *New J. Phys.*, 2011, **13**, 045020.
28. D. Zhang, A. H. Chai, X. H. Wen, L. L. He, L. X. Zhang and H. J. Liang, *Soft Matter*, 2012, **8**, 2152.
29. S. O. Nielsen, C. F. Lopez, G. Srinivas and M. L. Kleinn, *J. Phys. Condens. Matter*, 2004, **16**, R481.
30. C. W. Hsu and Y. L. Chen, *J. Chem. Phys.*, 2010, **133**, 034906.
31. W. L. Jorgensed, *J. Am. Chem. Soc.*, 1981, **103**, 335.
32. W. L. Jorgensen, J. Chandrasekhar and J. D. Madura, *J. Chem. Phys.*, 1983, **79**, 926.
33. S. J. Plimpton, *J. Comput. Phys.*, 1995, **117**, 1.
34. S. Nosé, *J. Chem. Phys.*, 1984, **81**, 511.
35. W. G. Hoover, *Phys. Rev. A*, 1985, **31**, 1695.
36. M. Deserno and C. Holm, *J. Chem. Phys*., 1998, **109**, 7678.
37. M. Deserno and C. Holm, *J. Chem. Phys*., 1998, **109**, 7694.
38. J. W. Eastwood, R. W. Hockney and D. N. Lawrence, *Comput. Phys. Commun.*, 1980, **19**, 215.
39. T. Wocjan, K. Klenin and J. Langowski, *J. Phys. Chem. B*, 2009, **113**, 2639.
40. M. L. Bennink, S. H. Leuba, G. H. Leno, J. Zlatanova, B. G. de Grooth and J. Greve, *Nat. Struct. Biol.,* 2001, **8**, 606.
41. G. Zifferer, *J. Chem. Phys.,* 1995, **102**, 3720.
42. G. Zifferer, *J. Chem. Phys.,* 1998, **109**, 3691.
43. J.Y. Su, L. X. Zhang, H. J. Liang, *J. Chem. Phys.,* 2008, **129**, 044905.
44. X. H. Wen, D. Zhang, L. X. Zhang, *Polymer,* 2012, **53**, 873.
45. Z. Y. Yang, D. Zhang, L. X. Zhang, H. P. Chen, A. Rehman and H. J. Liang, *Soft Matter,* 2011, **7**, 6836.
46. Y. Liu and B. Chakraborty, *Phys. Biol.,* 2008, **5**, 026004.
47. Y. T. Chen, Q. Zhang and J. D. Ding, *J. Chem. Phys.,* 2006, **124**, 184903.
48. S. Mogurampelly, B. Nandy, R. R. Netz and P. K. Maiti, *Eur. Phys. J. E*, 2013, **36**, 68.

49. A. Y. Grosberg, T. T. Nguyen and B. I. Shklovskii, *Rev. Mod. Phys.,* 2002, **74**, 329.

50. R. Messina, *J. Chem. Phys.*, 2002, **117**, 11062.

51. M. M. Hatlo and L. Lue, *Soft Matter*, 2008, **4**, 1582.

52. J. Lyklema, *Colloids Surf. A,* 2006, **291**, 3.

Figure Captions

Figure 1 Typical snapshots of DNA-nanosphere complex mixed with (a) monovalent anion M^{1-}, (b) divalent anion M^{2-}, (c) trivalent anion M^{3-}, and (d) tetravalent anion M^{4-}. Here, the anion concentration C_s=30.5mM (left column, a1-d1), 61.0mM (middle column, a2-d2), and 91.5mM (right column, a3-d3), respectively.

Figure 2 The percentage of DNA monomers wrapping around the nanoshpere, $< P >$, as a function of C_s for monovalent, divalent, trivalent, and tetravalent anions, respectively.

Figure 3 (a) Characteristic ratio of mean-square radius of gyration $< R_G^2 > / N_D l_0^2$ and (b) shape factor $< \delta >$ of double-stranded DNA as a function of C_s for monovalent, divalent, trivalent, and tetravalent anions, respectively.

Figure 4 $\vec{u}(1) \cdot \vec{u}(s)$ as a function of double-stranded DNA monomer *s* for different anion concentrations C_s of tetravalent anions M^{4-} (a) and for various anions with a fixed concentration C_s=91.5mM (b). Here 'isolated' means that there are only a DNA and a few cations for preserving the neutrality of the whole system.

Figure 5 Dihedral angle θ as a function of double-stranded DNA monomer *s* for different concentrations C_s of tetravalent anions M^{4-}.

Figure 6 Orientational correlation function $G(m)$ as a function of monomer interval *m* in

DNA for different concentrations C_s of tetravalent anions.

Figure 7. The integrated charge distribution, $Q_e(r)$, around the nanosphere for various anions with a fixed concentration C_s=91.5mM of DNA solutions (a) and DNA-absence solutions (b). The inset figure shows the $Q_e(r)$ of tetravalent anions M^{4-} with various concentrations C_s in DNA solutions.

Figure 8. (a) A schematic illustration of sphere shell in which DNA is located at $\phi \approx 0^\circ$ in the spherical coordinate and σ_e is the surface charge density in the local sphere shell whose angle is from $\phi - 18^\circ$ to $\phi + 18^\circ$ and whose radius is less than 26σ. σ_e as a function of ϕ for monovalent anion M^{1-} (b) and tetravalent anion M^{4-} (c), respectively. Left column C_s=30.5mM and right one C_s=91.5mM.

Figure 9. (a) σ_e as a function of ϕ at different simulation times for tetravalent anion M^{4-} with a fixed concentration C_s=91.5mM. Possible aggregation process for anions is shown in the inset figure. (b) The total deviations of integrated surface charge density *A* as a function of simulation time *t* for various anions with a fixed concentration C_s=91.5mM.

Figure 10. Typical snapshots of DNA-nanosphere complex mixed with (a) monovalent anion M^{1-}, (b) divalent anion M^{2-}, (c) tetravalent anion M^{3-}, and (d) tetravalent anion M^{4-} for the same cation concentration ($C_S^{'}$=465 mM).

Fig. 1

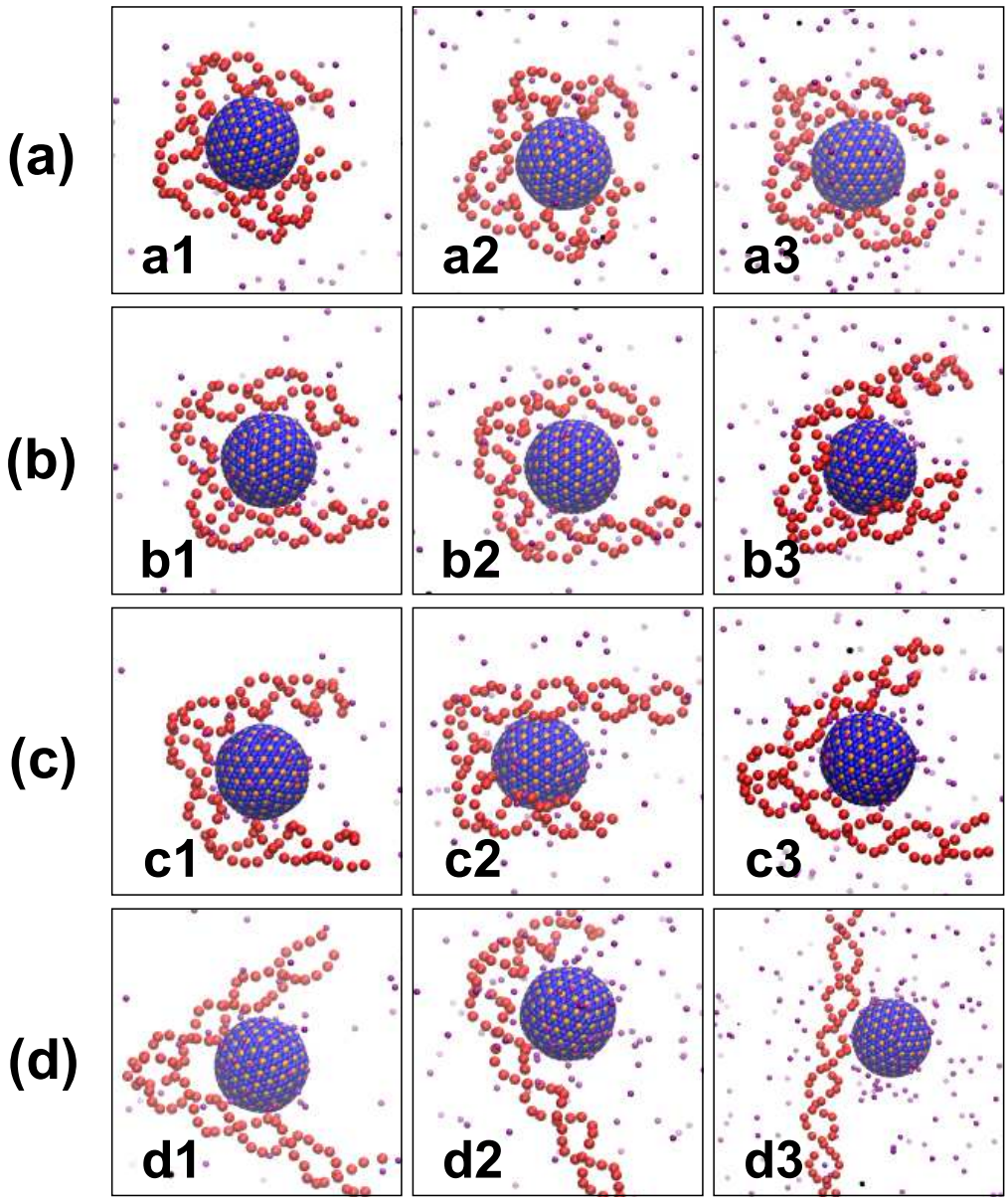

Submitted to *Soft Matter*

Fig. 2

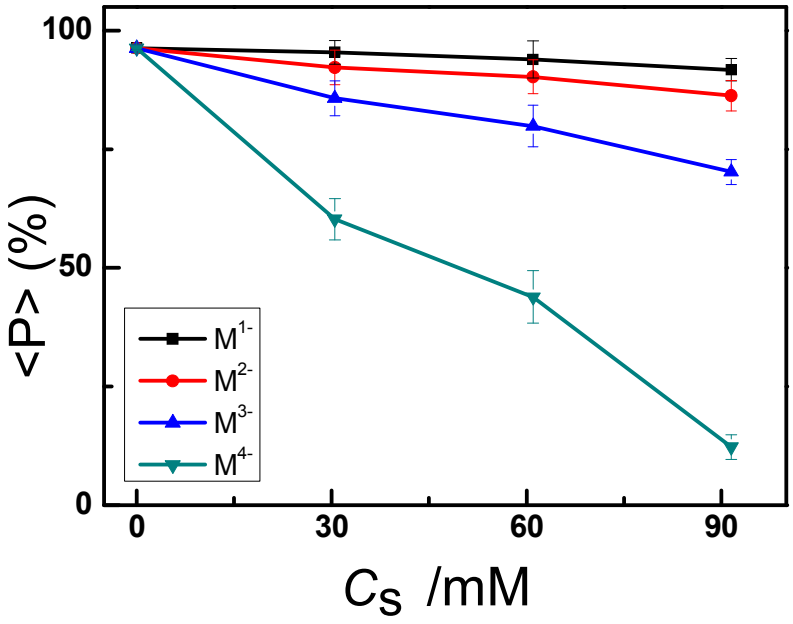

Fig. 3a

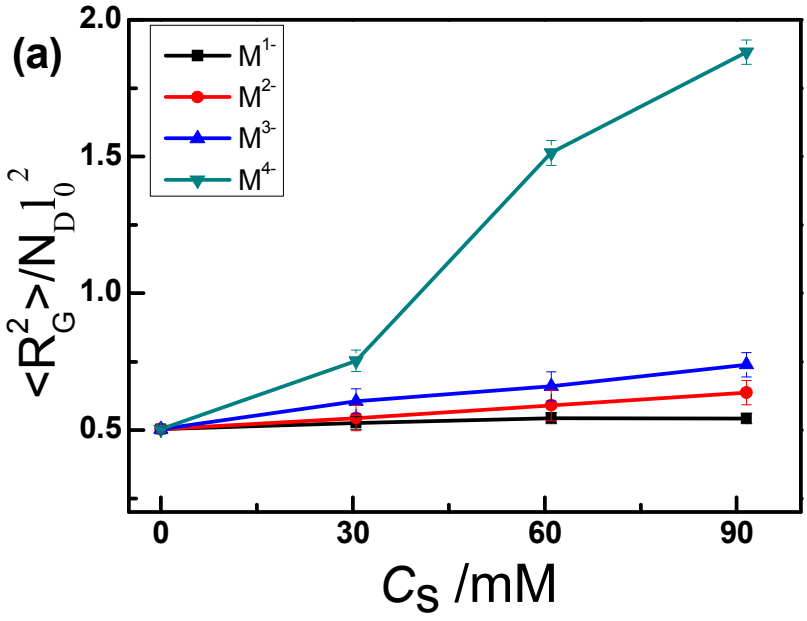

Submitted to *Soft Matter*

Fig 3b

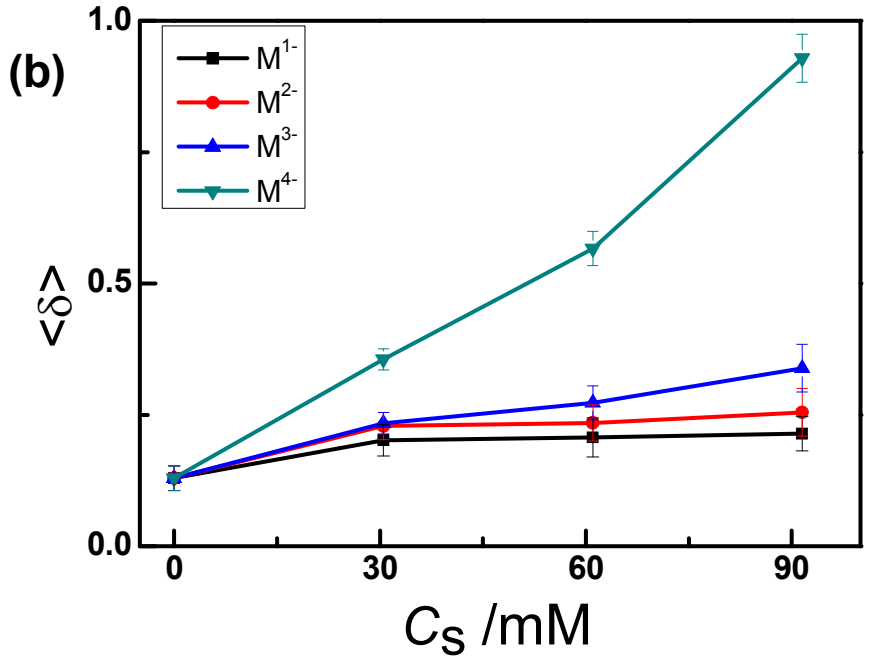

Submitted to *Soft Matter*

Fig. 4a

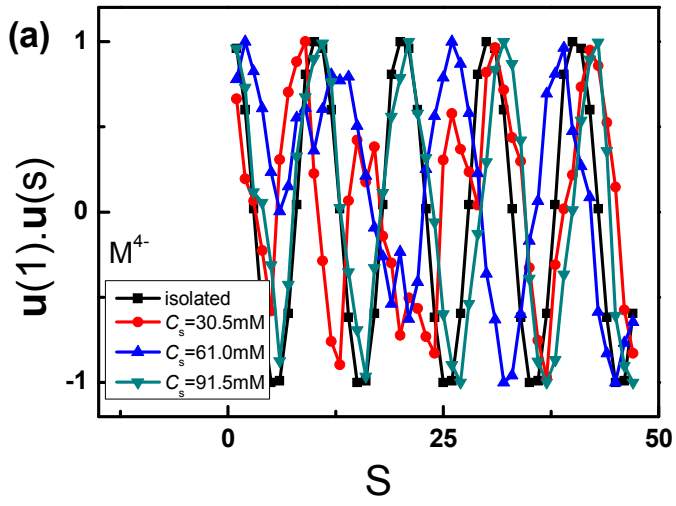

Submitted to *Soft Matter*

Fig 4b

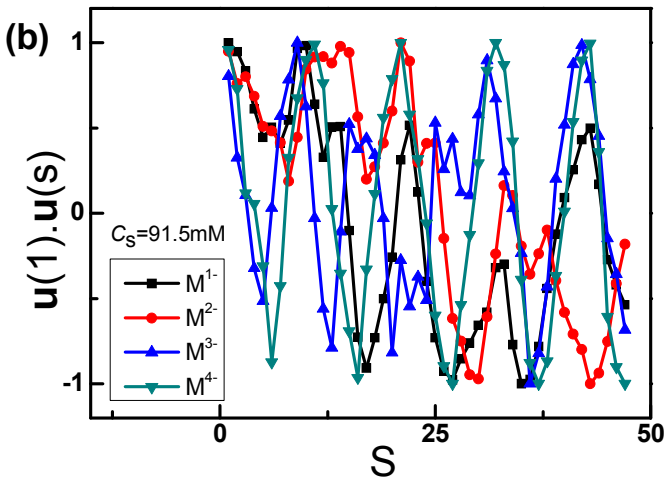

Submitted to *Soft Matter*

Fig. 5

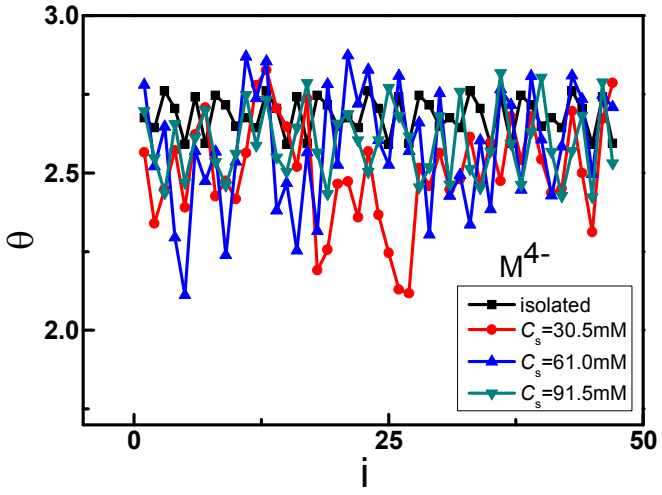

Submitted to *Soft Matter*

Fig. 6

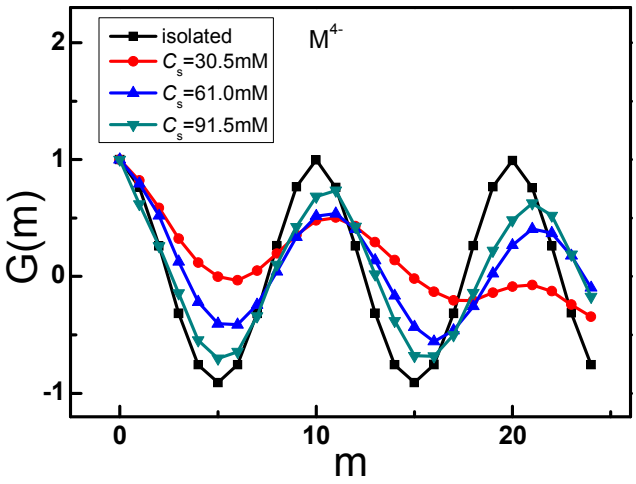

Fig. 7a

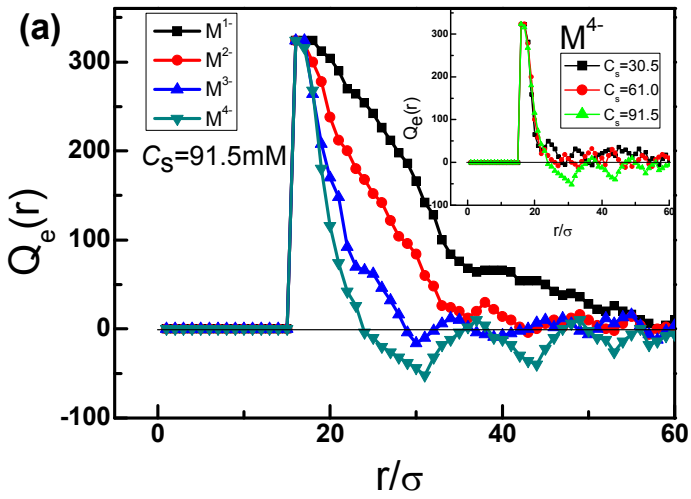

Submitted to *Soft Matter*

Fig 7b

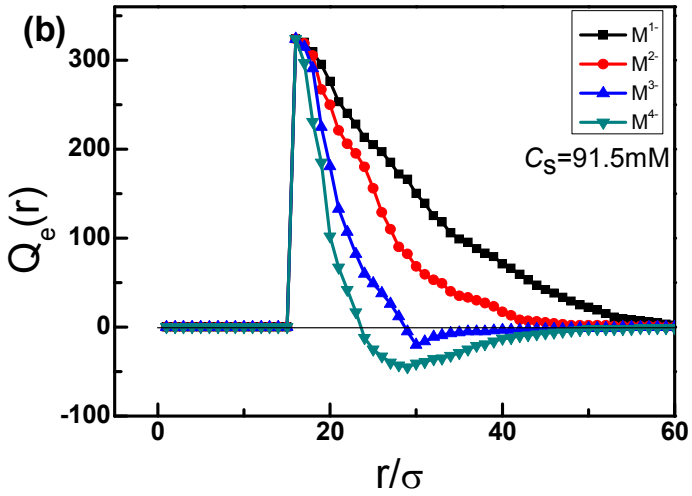

Fig. 8

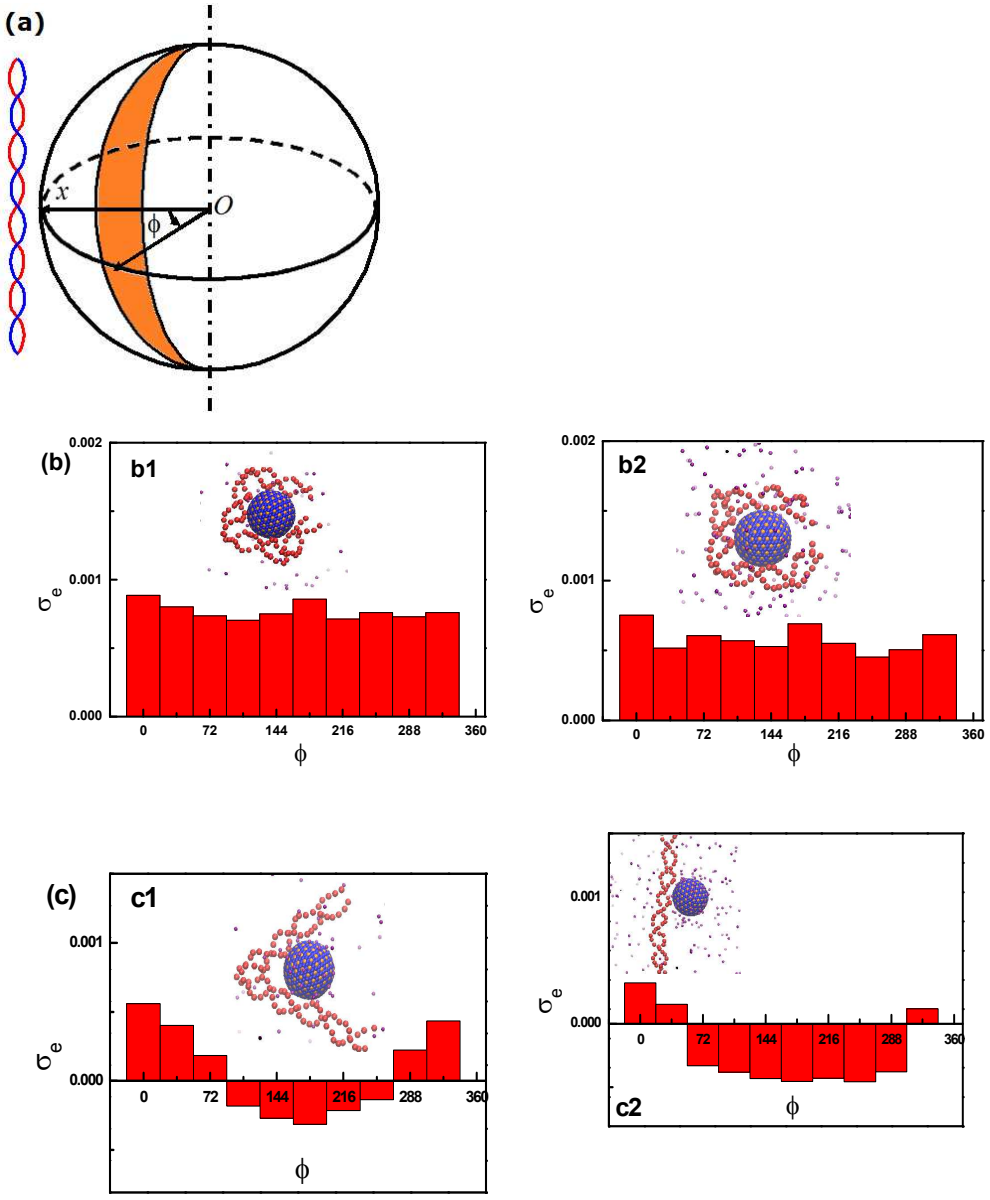

Submitted to *Soft Matter*

Fig. 9

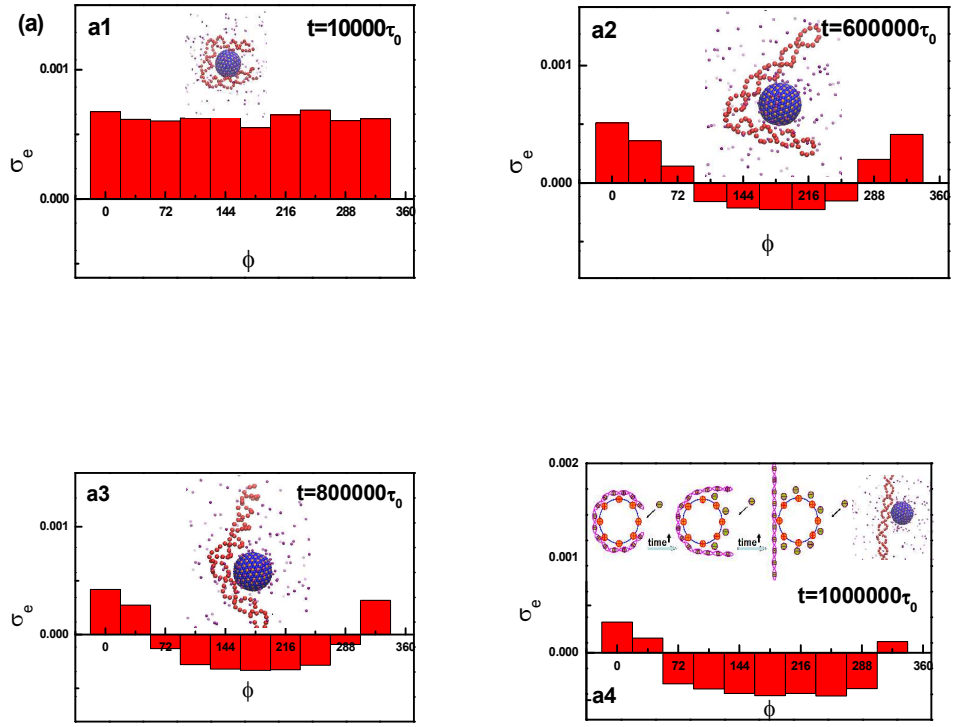

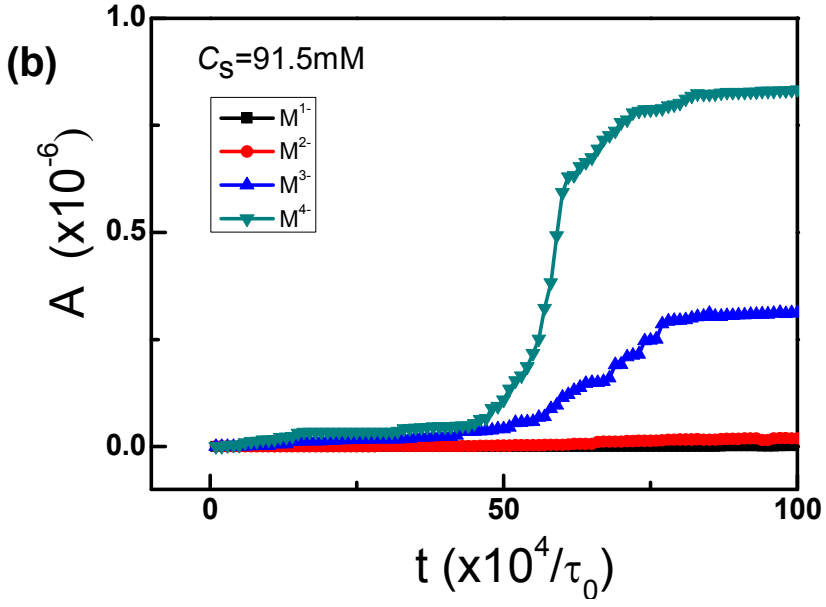

Submitted to *Soft Matter*

Fig. 10